DEVELOPMENT OF A FINITE ELEMENT MODEL OF 5TH PERCENTILE FEMALE WITH MULTIPLE MUSCLES AND ITS APPLICATION TO INVESTIGATION ON IMPACT RESPONSES OF ELDERLY FEMALES

Masami Iwamoto
Yuko Nakahira
Hideyuki Kimpara
Toyota Central R&D Labs. Inc.
Japan
Kyuengbo Min
Tokyo Metropolitan Institute of Medical Science
Japan
Paper Number 13-0366

ABSTRACT

The rates of fatality and injured persons of elderly people are gradually increasing in automotive accidents in Japan. In particular, elderly female occupants are most susceptible to injuries, especially on thorax and head-neck regions, based on previous studies using automotive accident data. This study developed a finite element (FE) model of 5th percentile female (AF05) with multiple muscles, and applied it to investigation on the injury mechanisms of elderly female occupants.

Individual muscle models of whole body with passive and active properties were integrated with an AF05 FE model that we developed previously. Material properties of skeletal parts with low strength of elderly people and smaller physiological cross-sectional area (PCSA) of each muscle of elderly females were obtained from the literature and commercially available image data, and were inputted to the model. Smaller PCSA of each muscle in elderly females would generate less muscular forces than younger males while less stiff bone properties of elderly females would generate more bone fractures than younger males. The developed elderly AF05 model without muscle activation was firstly validated against some cadaver test data on frontal impacts for the thorax and abdomen, and head-neck responses during a low-speed rear-end collision, and were compared with young adult 50th percentile male (AM50) model with multiple muscles that we developed previously. The simulation results of the elderly AF05 model generally showed good agreement with test data.

The elderly AF05 model was secondly used for investigation on effect of muscle activation to thoracic deformation in frontal impact situations with belt and hub loadings, and head-neck response in a low-speed rear impact situation. In the simulations on the thoracic deformation, a bracing condition was assumed and an activation level of 20% was assumed for all muscles in the trunk. Simulation results showed that the maximum thoracic deflections of the elderly AF05 model without muscle activation were two times and three times larger than those of young adult AM50 model with muscle activation in belt and hub loadings, respectively. From comparison between the elderly AF05 model and the young adult AM50 model, lower strength of bones and smaller PSCA of each muscle in the elderly AF05 model could increase thoracic deflection. In the simulation on the head-neck response, activation level of each muscle during a low-speed rear impact was estimated using a controller of multiple muscles with reinforcement learning (RL) that we developed previously. Simulation results showed that the maximum head angular velocity of the elderly AF05 model was larger than that of the young adult AM50 model, especially in considering muscle activation. The elderly AF05 could not prevent the head from rotating rearward due to their weak muscular forces.

Although the elderly AF05 model has some limitations on lack of experimental data for validations and estimation of muscle activation, it has the potential for better understanding of injury mechanisms of elderly female occupants.

INTRODUCTION

In Japan, population rate of elderly people more than 65 years old became over 23 % of total population in 2010 and is estimated to be increased for 40 % in 2060 (National Institute of Population and Social Security Research, 2012). The number of car accidents involving elderly drivers would increase at an accelerated pace with the increase in population of elderly people and elderly drivers' licensees, and is estimated to be beyond 2,100,000 and the social cost is estimated to be about 10 billion dollars 20 years later (The General Insurance Association of Japan, 2004). The Institute for Traffic Accident Research and Data Analysis (ITARDA) in Japan investigated traffic accident data on belted drivers from 2004 to 2006, and showed that fatality and serious injury rates increase with increase of age, and the fatality

rate of elderly drivers was about two times higher than that of younger adult drivers. The primary injury location was thorax and the secondary injury location was head-neck region, and the succeeding injury location was lower extremity in elderly drivers (ITARDA, 2007). Yee et al. (2006) investigated injury pattern of elderly victims more than 65 years old involved in motor vehicle collisions using data from Victorian State in Australia from 2001 to 2003. They reported that the most common injury for elderly victims was thoracic injury including multiple rib fractures and the second most common injury was head or neck injury.

According to NASS-CDS data analysis from 1993 to 2004 performed by Liu et al. (2007), the percentage of driver overall severe injury severity (MAIS4-MAIS6) of elderly females was 1.6 times higher than that of elderly males. The trend seems to be significant in belted front passengers. Based on accident data analysis in Japan performed by Yaguchi et al. (2011), the fatality of belted front passengers of elderly female was 3.6 times higher than that of elderly male while serious injuries of belted front passengers of elderly female was five times higher than that of elderly male. Augenstein et al. (2011) reported that elderly females sustained more severe injuries than elderly males for belted front seat occupants in frontal crashes based on accident data analysis using the 2000-2009 NASS/CDS data. Therefore, elderly female occupants have a tendency to sustain more fatal and severe injuries than elderly male occupants.

Brumbelow et al. (2009) investigated injury patterns in frontal crashes of vehicles based on the NASS-CDS crash data. They showed that occupants of 60 years old or older more often received at least one serious chest injury than a serious head injury, and the opposite was true for occupants younger than 30 years old. Simamura et al. (2003) conducted accident data analysis of a total 246 vehicle occupants using ITARDA data. They reported that elderly occupants frequently experienced rib fractures near the seatbelt line even under lower impact severity while younger occupants appeared not to sustain rib fractures even in higher impact collisions. These accident data analyses on thoracic injury indicate that elderly occupants tend to sustain thoracic injury differently from younger occupants. However, the thoracic injury mechanism of elderly occupants is not clear.

Krafft et al. (2003) investigated difference in the risk of permanent whiplash injury between males and females for different seating positions in rear impacts based on accident data reported to the Swedish insurance company Folksam during 1990-1999. The risk of permanent disability was three times higher for female drivers than male drivers. Similarly, permanent disability was 1.5 times higher for female front seat passengers and more five times higher for female rear seat passengers. Brolin (2003) performed a study of hospital data on neck injuries mainly due to fall and traffic accidents among the elderly in Sweden between 1987 and 1999. They showed that elderly have a death rate for cervical fractures that is three times higher than the death rate for the entire population. The fracture locations were mostly Atlas (C1) and Axis (C2) for elderly while those were mostly C4-C6 for younger population. Malik et al. (2008) analyzed the morbidity, mortality, and outcome of cervical spine injuries in 107 patients over the age of 65 years, which were caused by falls or road traffic accidents. They reported that cervical spine injuries are frequent in the elderly population. The injury patterns in elderly patients are different from those among younger patients. In addition, the injuries have the potential to influence the spinal cord and can result in death and permanent disability. Snyder et al. (1975) investigated basic physical measurements related to susceptibility to cervical hyperextension-hyperflexion injury. They found that the small elderly female was most susceptible to injury since the neck muscles are not strong enough even when fully tensed, to prevent the head from reaching its motion limit. However, the neck injury mechanism of elderly people, especially small elderly females, is not well known.

Many researchers investigated physical and motor functional characteristic features of elderly people. Bone mass or density is lost with age, especially in women after menopause so that bones become more brittle and may break more easily. The trunk becomes shorter as the disks gradually lose fluid and become thinner. The joints become stiffer and less flexible due to loss of fluid and cartilage in the joints (Bougie et al. 2001, Rosen et al. 1999). The physiological cross-sectional areas (PCSA) and strength of muscles decrease with age, and changes in the muscle tissue cause muscles to have less tone and ability to contract, even with regular exercise. In addition, muscle activation latency of elderly people is significantly larger than that of younger adults. Therefore, poor posture stabilization is found in elderly people during standing and sitting, especially in dynamic environments.

There are many studies using computational human body models to investigate mechanism of bone fractures of elderly people during automotive accidents (e.g. Ito et al.2009, El-Jawahri et al., 2010). In most of the studies, only loss of bone density and strength, and changes of bone shape with age were considered in their computational models developed to investigate the mechanism. However, recent studies showed that muscle activity before impacts is not negligible (Begeman et al. 1980, Ejima et al. 2009).

Computational human models are effective tools to

understand the injury mechanisms in automotive crashes. Recently, some human FE models have been developed with active muscles to investigate the muscular effects for human body kinematics. Behr et al. (2006) developed a FE model of the lower limb with 20 independent muscle bundles in the superficial and deep layers and used to investigate the effect of muscle tense on the skeletal injuries of the lower limb. They validated the model for isolated muscle contribution in the direction of fibers and bracing conditions under an emergency braking. Their simulation results indicated that muscle activation in bracing during frontal impacts significantly increased the stress level on the tibial shaft. Authors also developed a finite element model of human whole body with multiple muscles (Iwamoto et al. 2011). Simulation results using the human model showed that muscular forces before impacts could affect injury outcomes significantly. In addition, authors showed that muscle activation and the control have an important role on body posture stabilization in impact situations (Iwamoto et al. 2012). Therefore, the loss in PCSA of each muscle and poor ability of posture stabilization in elderly people are supposed to affect kinematics and injury outcomes of elderly drivers and passengers.

In this study, we newly developed a small female FE model with multiple muscles to investigate how age-related ability in muscular forces could affect injury outcomes of elderly female occupants. The developed model was firstly validated against cadaver test data on thoracic and head-neck responses during impacts. The developed model was secondly used for investigation on effect of muscle activation to thoracic deformation in frontal impact situations, and head-neck response in a low-speed rear impact situation. We investigated effects of loss in muscular forces of elderly people for kinematics and impact responses of the human body. All simulations in this paper were performed using an explicit finite element code LS-DYNA (LSTC, USA).

DEVELOPMENT OF ELDERLY SMALL FEMALE FE MODEL

A human whole body FE model with muscles

In previous studies, we developed muscular FE models of a human whole body and integrated them with a human body FE model called THUMS (Total HUman Model for Safety, Iwamoto et al. 2002) whose size was similar to that of AM50 with a height of 175 cm and a weight of 77 kg (Iwamoto et al. 2011 and 2012). Each muscle model of the AM50 model was scaled down to adjust the size of AF05 (5th percentile female) with a height of 152 cm and a weight of 46 kg, and was incorporated into an AF05 FE model that we developed previously (Kimpara et al. 2005 and Iwamoto et al. 2007). Figure 1 shows a developed small female FE model with multiple muscles. In this figure, the skin was removed to see muscles clearly. The model includes 266 muscles of lower extremities, upper extremities, trunk, and neck such as the Sternocleidmastoid, Trapezius, Rectus Abdominis, Erector Spinae, Pectoralis Major, Deltoid, Biceps Brachii, Triceps, Extensor Digitorum, Flexor Carpi Radialis, Rectus Femoris, Gluteus Maximus, Vastus Medialis, Biceps Femoris, Vastus Lateralis, Tibialis Anterior, Gastrocnemius, and so on. Total number of nodes and elements in the whole body model is about 140,000 and 240,000, respectively.

Each muscle FE model was represented as a hybrid model by combination of solid elements with passive muscle properties and bar elements with active muscle properties. The solid elements were modeled with a rubber-like material model (LS-DYNA: #181, MAT_SIMPLIFIED_RUBBER) to simulate 3D geometry of individual muscles and non-linear passive properties. This material model is based on Ogden model and users can use the model by inputting a single uniaxial non-linear stress-strain curve. Poisson's ratio is set to 0.495. The non-linear passive properties were given using tensile properties of muscles obtained from Yamada (1970). The bar elements were modeled with a Hill type muscle model (LS-DYNA: #156, MAT_MUSCLE) to generate muscular force according to inputted activation levels which are in a range from 0 to 1. Some material properties are needed for the Hill type muscle model. A maximum contraction force per unit cross-sectional area of 5.5 kgf/cm^2 of each muscle was obtained from Gans (1982). The active force-length and active force-velocity curves were obtained from Thelen et al. (2003). Although the passive force-length relations are needed in the Hill

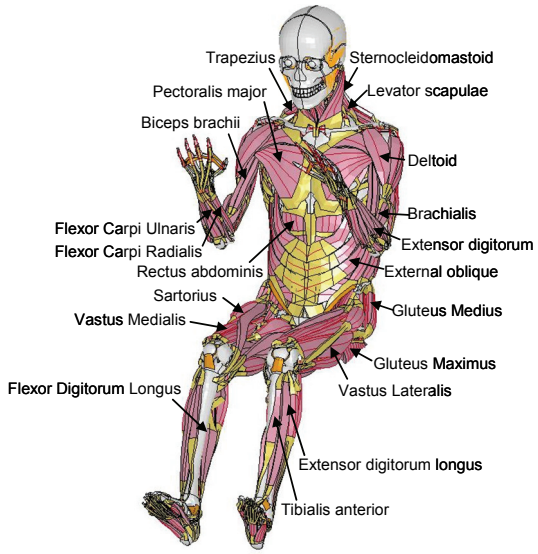

Figure 1. A small female FE model with muscles.

type model, they were not assigned to bar elements because the solid elements have the passive properties. According to anatomical text (Agur et al., 2005), each muscle model was connected to the corresponding bone model through tendon models. The tendons were modeled by using shell or solid elements at both ends of muscles. Material properties of the tendons were obtained from the literature (Pioletti et al., 1998, Carlson et al., 1993). Some sliding contacts were defined to produce the interaction between adjacent two muscles and the interaction between muscles and bones close to the muscles. The skin was modeled using shell elements with elastic material properties obtained from Yamada (1970) while the fat was modeled using solid elements with the rubber-like material model. Sliding interfaces were also defined to produce interaction between the muscles and the skins.

Aging effects in material properties

PCSA data of muscles for elderly people Force generated by a single muscle is proportional to its PCSA. Therefore, the PCSA of each muscle could affect the muscular force significantly. The PCSA of each muscle model was primarily determined based on Winters (1990). The PCSA data of one third of all muscles were determined based on two series of physical slicing data with high resolution of a 38 years old adult male cadaver with a height of 180 cm and a weight of 90 kg, and a 59 years old elderly female cadaver with a height of 167cm and a weight of 72 kg. These image data were obtained from commercially available data (Visible Human Project Data; NIH, USA). Table 1 shows PCSA data of primary muscles in the adult male and the elderly female, and rate of each PCSA of the elderly female against that of the adult male. The obtained PCSA of each muscle in the elderly female was inputted as cross-sectional area of bar elements with active muscle properties of the corresponding muscle in the small female FE model. The muscular PCSAs of the elderly female were smaller than those of the adult male and the rates of muscular PCSAs of the elderly female against those of the adult male were from 13 to 84 % (average value: 51 %).

Material properties of ribcage for elderly people According to accident data analysis described previously (ITARDA 2007, Yee et al. 2006), the primary skeletal injury locations were thorax and lower extremity in elderly occupants. Therefore, we focused on the ribcage and long bones of lower extremity in determining bone properties of the elderly female model. As for aging effect in material properties of the rib, Kemper et al. (2005) measured tensile properties of cortical bones in ribs using six cadavers including three females with 46, 61, and 64 years old and three males with 18, 45, and 67 years old. Figure 2(a) summarizes tensile stress-strain curves of rib cortical bones obtained from Kemper et al.. The elastic moduli of ribs in elderly females were stiffer than those in the youngest male while the failure strains of ribs in elderly females were half as much as those in the youngest male. We inputted the average values of material properties of the elderly females as material properties of ribs in the small female FE model.

Table 1.
PCSA* data of primary muscles in adult male and elderly female

Body Part	Muscle Name	PCSA* A (mm^2)		Ratio
		Young male A_{ym}	Elder female A_{ef}	A_{ef}/A_{ym} (%)
Neck	Sternocleidomastoid	166.00	131.50	79.22
	Longus Colli	39.30	25.90	65.90
	Splenius Capitis	99.00	75.40	76.16
	Semispinalis Capitis	95.20	50.40	52.94
Shoulder	Levator Scapulae	993.00	125.70	12.66
	Trapezius	2323.00	868.50	37.39
	Deltoid	2282.00	1455.40	63.78
	Pectoralis Major	1179.00	872.08	73.97
Upper Arm	Biceps Brachii	319.00	174.67	54.76
	Brachialis	881.00	247.67	28.11
Lower Arm	Flexor Carpi Ulnaris	557.00	129.17	23.19
	Extensor Digitorum	430.00	81.48	18.95
	Flexor Carpi Radialis	310.00	92.59	29.87
Abdomen	Rectus Abdominis	658.00	372.48	56.61
	External Oblique	685.00	439.86	64.21
Hip	Gluteus Medius	1710.00	1308.00	76.49
	Gluteus Maximus	1813.00	1458.00	80.42
Upper Leg	Sartorius	320.00	268.00	83.75
	Vastus Medialis	3237.00	1560.00	48.19
	Vastus Lateralis	4063.00	1648.00	40.56
Lower Leg	Tibialis Anterior	1277.00	848.00	66.41
	Flexor Digitorum Longus	1897.00	586.00	30.89
	Extensor Digitorum Longus	667.00	404.00	60.57

*PCSA: physiological cross-sectional area

As for aging effect in material properties of the rib cartilage, Yamada (1970) reported on tensile stress-strain curves of rib cartilages using 28 cadavers with ages from 20 to 69 years old. Figure 2(b) shows tensile stress-strain curves of rib cartilages obtained from Yamada. The elastic moduli of rib cartilages in elderly persons were less stiff than those in the young adult persons while the failure strains of rib cartilages in elderly persons were half as much as those in the young adult persons. These material properties were inputted into the ribcages in the small female FE model. The thickness of rib cortical bone in the small female FE model was set to the average value of elderly persons including males and females by referring to Kemper et al. (2005).

Material properties of long bones in lower extremities for elderly people As for aging effect in material properties of long bones of lower extremities, Yamada (1970) reported on tensile stress-strain curves of cortical bones of femur and tibia using cadavers with ages from 20 to 39 years old and those with ages from 60 to 69 years old as

shown in Figure 3. These data include male and female cadavers. The stresses in post-yield region and failure strains of elderly people is 20 % and 10 % lower than those of young adults, respectively. These material properties were inputted into the femur and tibia in the small female FE model.

In occupant models, bending mode is estimated to be dominant during frontal impacts because of axial compressive load from foot/ankle under a condition with entrapped knee for the tibia and fibula, and axial compressive load from instrumental panel under a condition with fixed pelvis for the femur. Therefore, we validated the long bone models for static 3-point bending tests of the long bones using 43 male or female cadavers with ages from 20 to 83 years old conducted by Yamada (1970). Figure 4 shows a simulation setup of static 3-point bending for the femur model, which reproduced the test condition.

Figure 5 shows comparison of load-deflection curves of the femur and tibia between simulation results and test data. These figures include simulation results of young adult AM50 model (Iwamoto et al. 2011) and

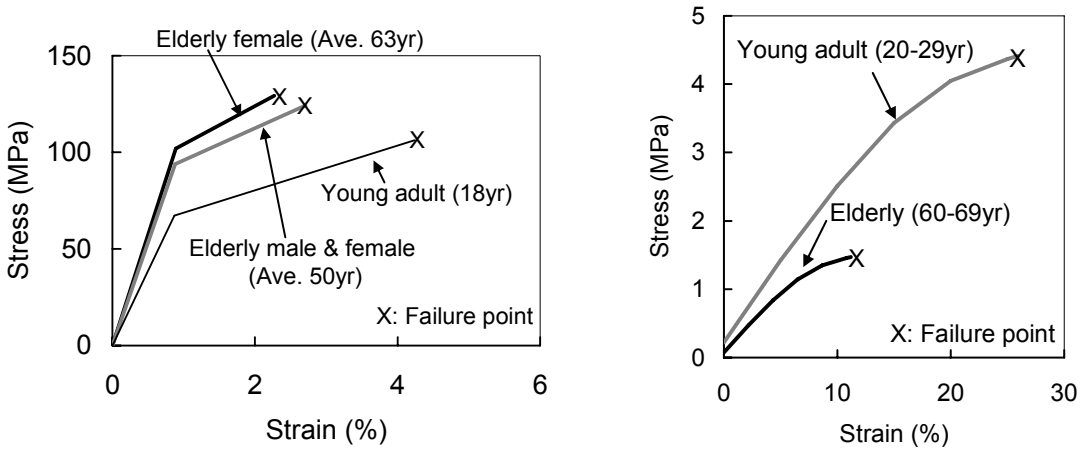

(a) Rib cortical bone (b) Rib cartilage

Figure 2. Tensile properties of rib cortical bone and rib cartilage.

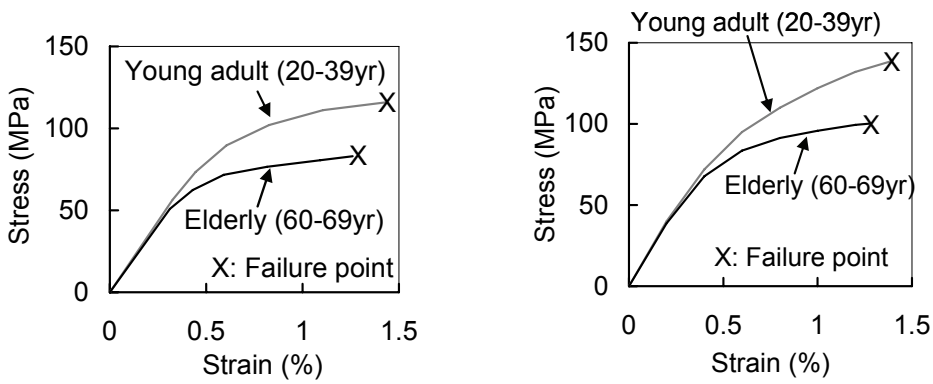

(a) Femur (b) Tibia

Figure 3. Tensile properties of cortical bones of femur and tibia.

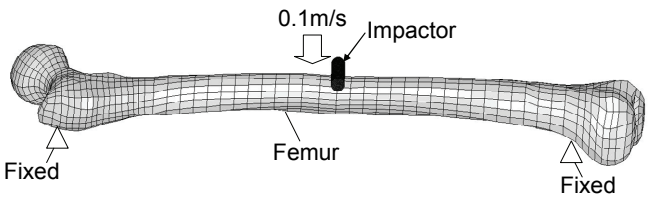

Figure 4. Simulation setup of static 3-point bending for the femur model.

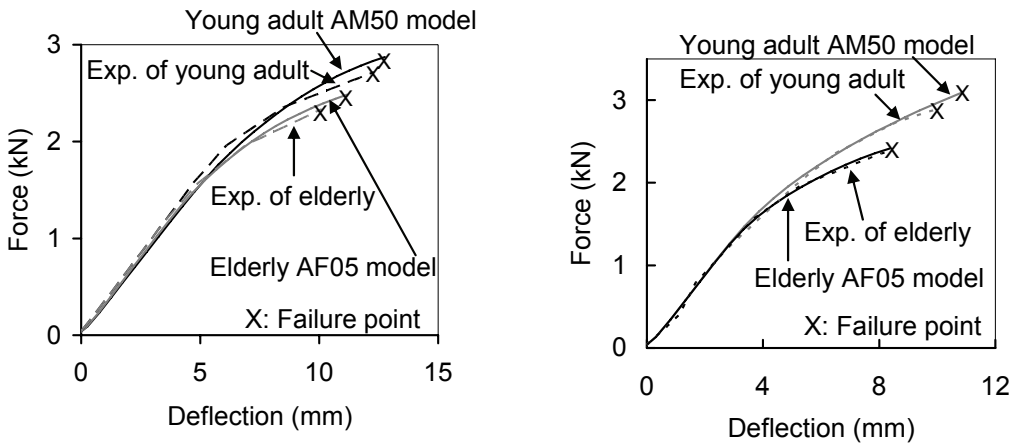

(a) Femur (b) Tibia

Figure 5. Comparison of load-deflection curves in 3-point bending between simulation results and test data.

elderly AF05 model. Simulation results of both models show good agreement test data except the failure deflection. The reason why the deflections at failure were different between simulation results and test data is probably because the material model of cortical bone did not have the anisotropy.

Material properties of cervical vertebral discs for elderly people As for aging effect in material properties of cervical vertebral discs, Yamada (1970) reported on stress-strain curves of wet intervertebral discs in tension. He showed that the elongation at the same stress is a little less in the 40-79 age group than in the 20-39 age group. Therefore, we inputted 1.23 times higher stiffness to C1-C7 discs in elderly AF05 model than in young adult AM50 model. In addition, Brolin (2003) reported on aging effect of mobile segments in cervical spine, and described that C1-C2 motion segment is the most mobile portion of the cervical spine for the normal elderly, as opposed to the C4-C7 motion segment in the younger population. Malik et al. (2008) indicated that the reason of the difference was that the C4-C7 segments would become stiffer with age so that the C1-C2 segment would become the most mobile portion of the cervical spine in elderly people. In this study, we inputted 1.3 times higher stiffness to C4-C7 discs for the elderly AF05 model, which had already had the abovementioned stiffness of cervical discs, to represent cervical spine motion of elderly people.

VALIDATION OF ELDELY SMALL FEMALE FE MODEL

In this study, we validated the elderly AF05 model against some cadaver test data to confirm if the model without muscle activity showed cadaveric responses. The model was validated against four sets of cadaver test data on thoracic and abdominal responses during frontal impacts, and head-neck motions during rear impacts, which were obtained from the literature (Kroell et al.1971, Kent et al. 2004, Nusholtz et al. 1988, White et al. 2009). In simulations of these validations using cadaver test data, muscle activation level of each muscle should be set to 0.0 (0 %) because cadaver has no muscle activity. However, in this study, we set the muscle activation level to values less than 0.01 (1.0%) to ensure computational stability.

Thoracic responses in frontal impacts

The developed elderly AF05 model was validated for frontal impact cadaver test data conducted by Kroell et al. (1971). Kroell et al. conducted a series of cadaver tests on thoracic frontal impacts. Their tests included two cadavers of which the anthropometric data were similar to those of AF05. In simulations, a 23.4 kg hub impactor hit frontal surface of the thorax at two speeds of 6.9 and 9.9 m/s in order to reproduce the experimental set-up (Figure 6(a)). Thoracic deflection was obtained from the distance between the impactor surface and the thoracic posterior surface. Figure 6(b) demonstrates predicted human behaviors in the frontal impact simulations. Figure 7 shows comparison of thoracic force-deflection curves between simulation results and test data at two impact speeds of 6.9 m/s and 9.9 m/s. These figures include two simulation results using young adult AM50 model and elderly AF05 model. Figure 7(a) also includes two elderly female cadaver test data. The simulation results with both impact speeds almost fell within cadaver test corridors. The maximum thoracic deflection of elderly AF05 model was lower than that of young adult AM50 model, and was close to the minimum deflection of the test corridors while the thoracic force until deflection of 30 mm of elderly AF05

model was lower than that of young adult AM50 model. These differences are probably because the body mass and thoracic thickness of the elderly AF05 model were smaller than those of the young adult AM50 model. Figure 8 shows stress distributions of the ribcage with bone fracture locations in the ribs and sternum of elderly AF05 model at the two impact speeds. The model predicted 13 rib fractures and 1 sternum fracture in the case of 6.9 m/s. In the cadaver tests, cadavers from 67 to 80 years old (average of 74.6) sustained 14.6 rib fractures and 1.2 sternum fractures in the case of 6.9 m/s. Therefore, the model has a possibility to predict bone fractures in the ribcages of elderly female occupants.

Kent et al. (2004) presented thoracic response corridors developed using fifteen post-mortem human subjects (PMHS) subjected to four loadings of single and double diagonal belt, distributed, and hub loading on the anterior thorax. Subjects were positioned supine on a table and a hydraulic master-slave cylinder arrangement was used with a high-speed materials testing machine to provide controlled chest deflection at a rate similar to that experienced by restrained PMHS in a 48 km/h sled

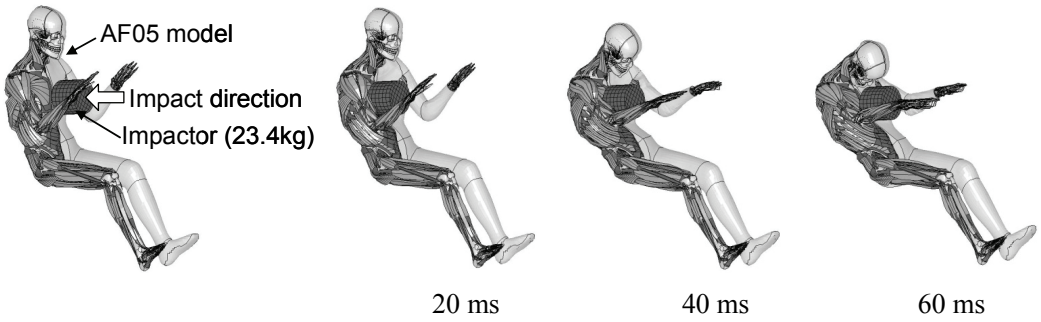

(a) Simulation setup (b) Impact behaviors (impact speed:6.9 m/s)

Figure 6. Hub impact simulation for thorax of elderly AF05 model.

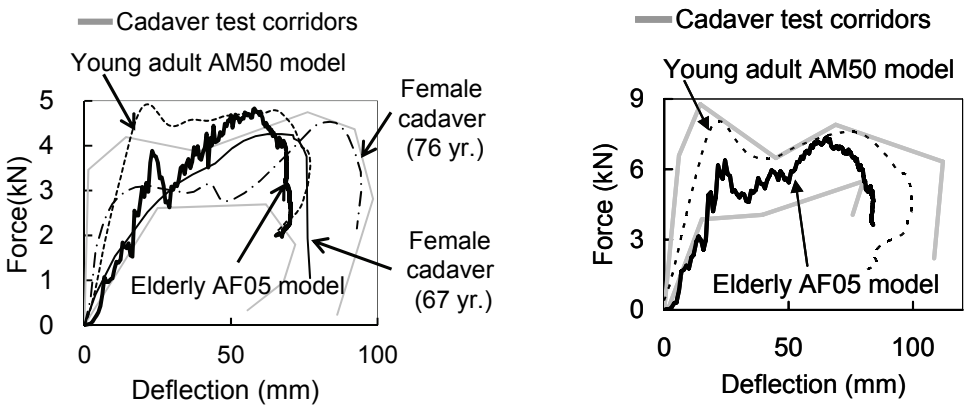

(a) 6.9 m/s (b) 9.9 m/s

Figure 7. Comparison of thoracic force-deflection curves between simulation results and test data.

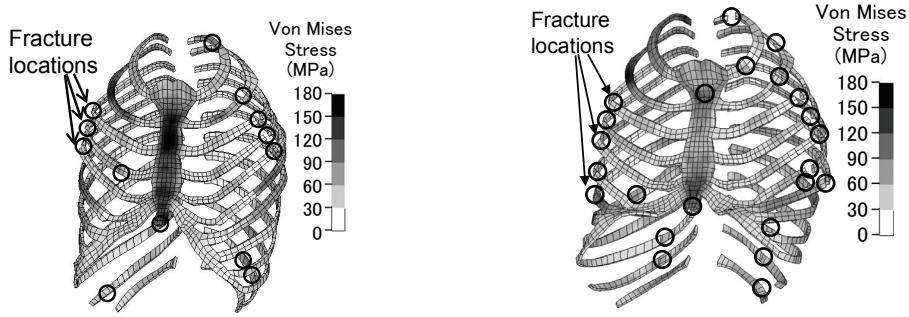

(a) 6.9 m/s (b) 9.9 m/s

Figure 8. Stress distributions of the ribcage with bone fracture locations of elderly AF05 model.

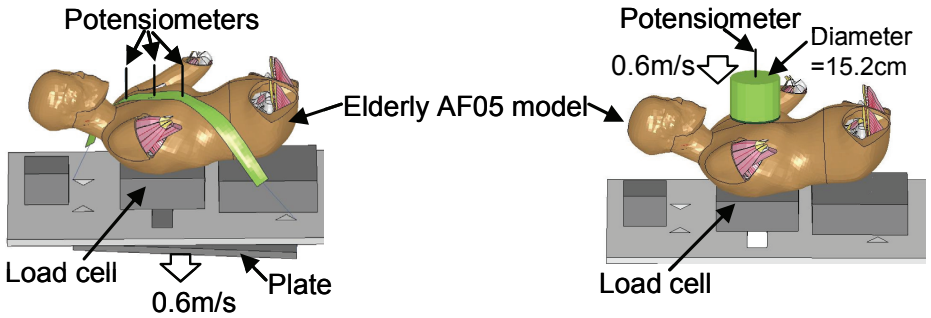

(a) Single shoulder belt (b) Hub impactor

Figure 9. Simulation setups for two cases of hub and single shoulder belt loadings.

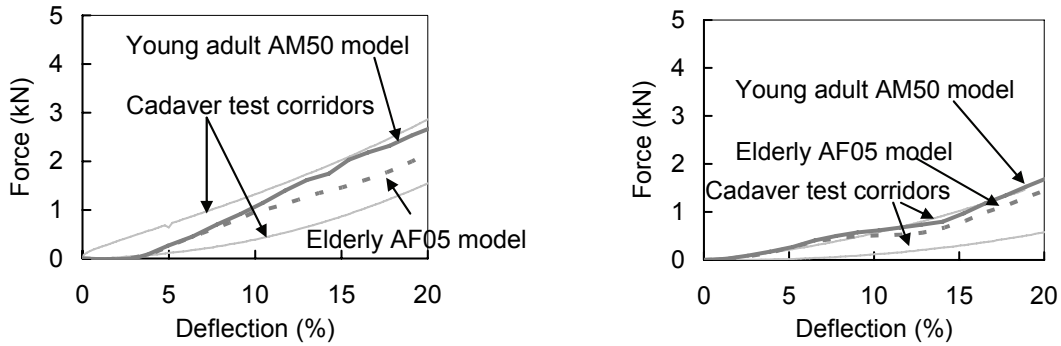

(a) Single shoulder belt (b) Hub impactor

Figure 10. Comparison of force-deflection curves in thorax between simulation results and test data.

test. Thoracic response was characterized using the deflection at the midline of the sternum and a load cell mounted between the subject and the loading table. Simulation setups using the human body FE model carefully reproduced the abovementioned experimental setups. Figure 9 shows simulation setups for the two cases of hub and single shoulder belt loadings. Figure 10 shows simulation results of the posterior reaction forces and chest deflection compared with test corridors. Simulation results generally fell within test corridors in both cases.

Abdominal responses in frontal impacts

Nusholtz et al. (1994) conducted abdominal frontal impact tests using three cadavers of a 63 years old male with a height of 180cm and a weight of 70.1 kg, a 46 years old male with a height of 176 cm and a weight of 50.0 kg, and a 55 years old female with a height of 162 cm and a weight of 70.3 kg. Figure 11(a) shows a simulation setup to reproduce the experimental cadaver tests, in which the impactor simulated a lower half of a steering wheel. In this simulation, the mass and initial velocity of the impactor were set to 18 kg and 10 m/s, respectively. Figure 11 (b) shows comparison of abdominal force-deflection curves between simulation results and test data. Predicted force-deflection curve of the elderly AF05 model was similar to that of the 55 years old female cadaver. The initial slope of the force-deflection curve of the elderly AF05 model was lower than that of young adult AM50 model. These differences are probably because the body mass and abdominal thickness of the elderly AF05 model were smaller than those of the young adult AM50 model.

Head-neck responses during rear impacts

The elderly AF05 model was validated against cadaver test data on head-neck responses during a low-speed rear impact. White et al. (2009) investigated head-neck responses during rear impact with a velocity of 8 km/h using two cadavers of a 41 years old male with a height of 180 cm and a weight of 99 kg and a 64 years old male with a height of 176 cm and a weight of 82 kg. They showed head C.G. (Center of Gravity) angle time histories of the cadavers. Ono et al. (1997) performed a series of volunteer tests to investigate head-neck responses during rear impact with the same velocity of 8 km/h as White et al. and with almost the same experimental conditions. In this study, we performed simulations to predict head-neck responses during the rear impact situation. The accelerations of X direction (posterior-anterior) and Z direction (inferior-superior) at T1 and angle time histories

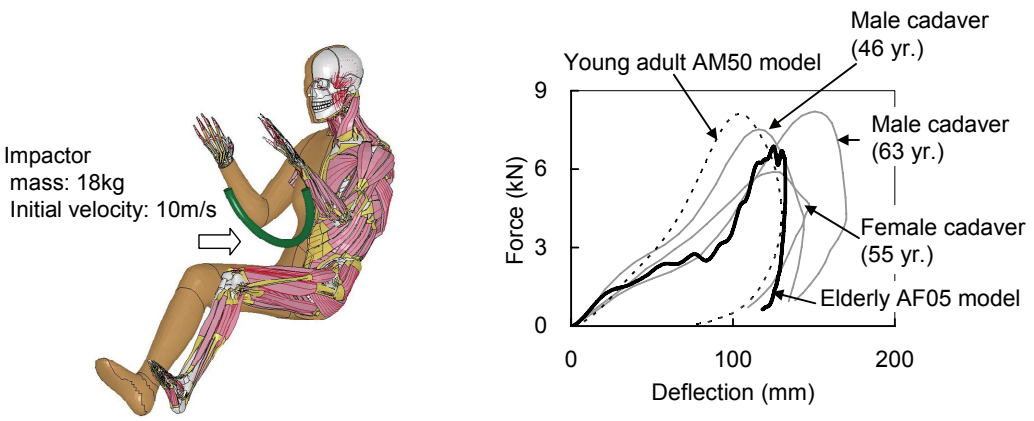

(a) Simulation setup (b) Force-deflection curves

Figure 11. Abdominal impact simulations using an impactor simulating a steering wheel.

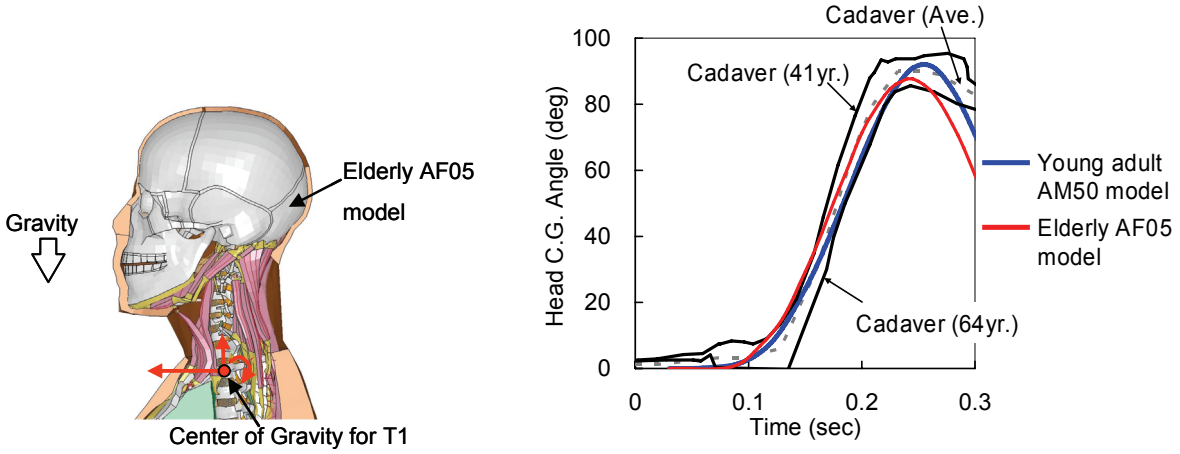

(a) Simulation setup (b) Comparison of head C.G. angle time histories

Figure 12. Low-speed rear impact simulations with a velocity of 8km/h.

around Y axis obtained from the volunteer tests were given to the T1 in two models of young adult AM50 model and elderly AF05 model. Figure 12(a) shows a simulation setup of the low-speed rear impact. Figure 12(b) shows comparison of head C.G. rotational angle between simulation results using the two models and experimental test data. The two simulation results show good agreement with cadaver test data, although there are some differences after peak head C.G. rotational angle. In addition, the peak head C.G angle of the elderly AF05 model was close to that of elderly cadaver (64 years old) while the peak head C.G angle of young adult AM50 model was close to that of the average angle-time history curve of two cadaver tests. Therefore, the elderly AF05 model has a possibility to simulate head-neck motions of elderly occupants during low-speed rear impacts.

AGING EFFECTS OF MUSCULAR FORCES FOR IMPACT RESPONSES

Aging effect of muscular forces for thoracic impacts

In emergency braking before an impact, well-trained drivers do braking by activating agonists and antagonists efficiently while beginner drivers do braking by activating both agonists and antagonists simultaneously. In the latter cases, the activation levels have a tendency to be larger than in the former cases. In this study, we hypothesized that drivers cannot control agonists and antagonists in the worst cases of emergency braking so that the activation levels of agonists and antagonists could be the same. We investigated how muscle activation levels could affect cadaveric impact responses for the thorax under the same simulation conditions conducted by Kent et al. (2004) and Kroell et al. (1971) described previously when drivers took the activation levels in the worst cases of emergency braking. The same muscle activation level was inputted to all agonist and antagonist muscles in the trunk under the same simulation conditions of the thoracic impacts. The

activation level was set to 0.2 (20 %), which was the average of activation levels of the trunk muscles or lower extremity muscles measured in the volunteer tests on driver's bracing that we conducted previously (Iwamoto et al. 2011).

Figure 13 compared thoracic force-deflection curves of simulation results with and without muscle activation under the thoracic impact conditions of Kent et al. (2004). The figure includes simulation results of the young adult AM50 model and the elderly AF05 model. In both models, the slope of force-deflection curve with muscle activation was larger than that without muscle activation. The muscle activation tends to increase the thoracic stiffness. In addition, the thoracic stiffness of the elderly AF05 model was much lower than that of the young adult AM50 model in the case with muscle activation. Figure 14 shows comparison of the maximum thoracic deflection at 1kN loading obtained from the force-deflection curves of Figure 13 between the young adult AM50 model and the elderly AF05 model. The maximum thoracic deflections of the elderly AF05 model without muscle activation was three times and two times larger than those of the young adult AM50 model with muscle activation in the cases of hub impactor loading and single shoulder belt loading, respectively. These results suggest that the elderly female occupants in passenger seats who are not easy to brace their bodies before impacts tend to have more thoracic deflection than young adult males in driver seats who are relatively easy to brace their bodies in frontal impacts. Figure 15(b) shows muscle tensing influence on peak force as a function of the maximum thoracic deflection in hub impactor loadings. The figure includes simulation results with a low-speed of 0.6 m/s for the impact condition of Kent et al. (2004) and a high-speed of 6.9 m/s for the impact condition of Kroell et al. (1971). Thoracic forces for thoracic deflections of 5, 10, 15, 20 % with and without activation were obtained as shown in Figure 15(a) and the percent increase of the force

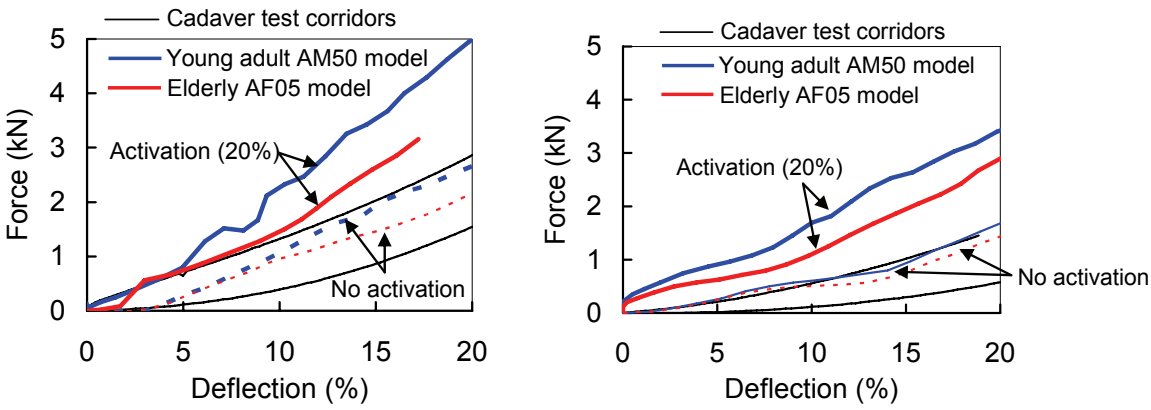

(a) Single shoulder belt (b) Hub impactor

Figure 13. Comparison of thoracic force-deflection curves of simulation results with and without muscle activation in thoracic impacts.

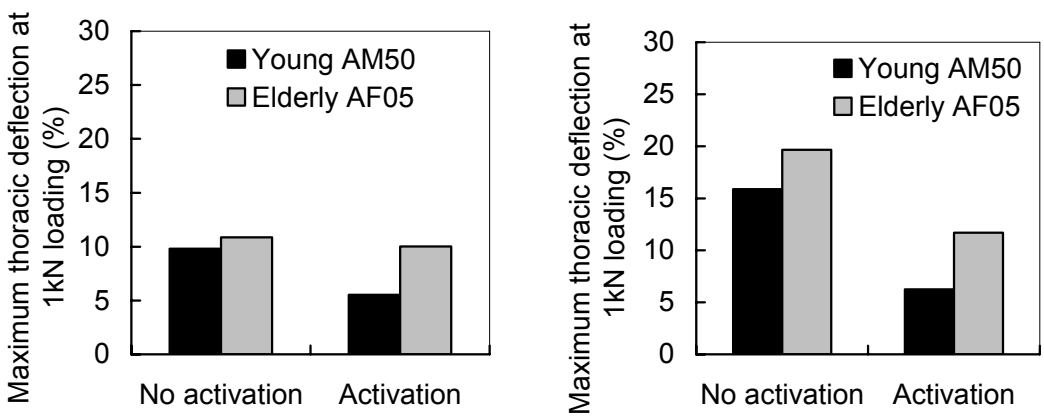

(a) Single shoulder belt (b) Hub impactor

Figure 14. Comparison of the maximum thoracic deflection at 1kN loading between young adult AM50 model and elderly AF05 model.

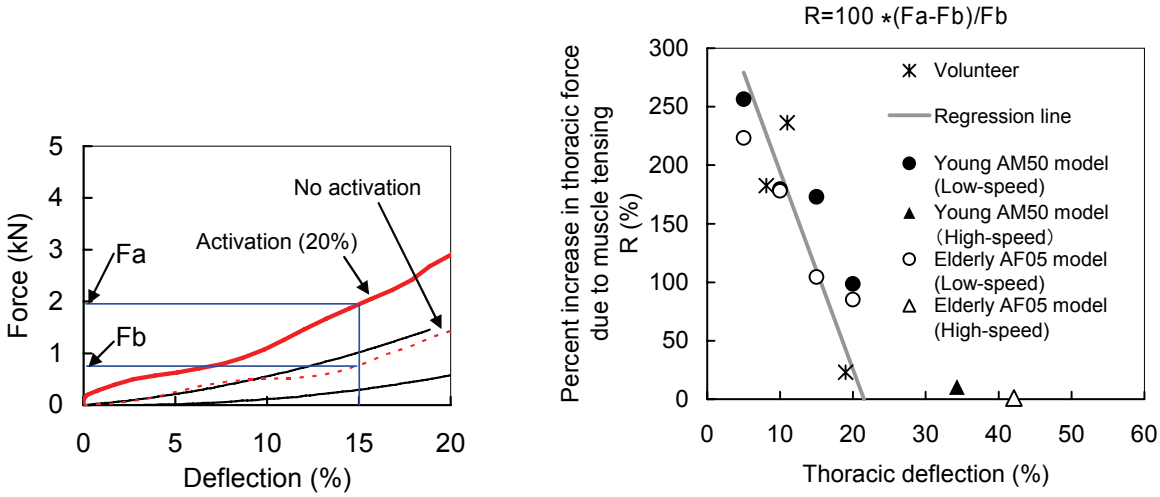

(a) Calculation method of percent increase (b) Comparison of percent increase in thoracic force

Figure 15. Muscle tensing influence on peak force as a function of the maximum thoracic deflection in hub impactor loadings.

with activation for the force without activation was calculated and plotted on the graph of Figure 15(b). The graph also includes human volunteer test data. The original human volunteer test data were obtained from Stalnaker et al. (1973). The percent increases of thoracic force due to muscle tensing predicted by both models of young adult AM50 model and elderly AF05 model were almost along the regression line in low-speed hub impactor loadings while the percent increase of thoracic forces predicted by both models were almost zero in high-speed hub impactor loadings. Therefore, the model has a possibility to estimate muscular effects on the thoracic impact responses.

Aging effect of muscular forces for head-neck responses during rear impacts

In rear impact scenarios of real-world accidents, the occupants are supposed to activate their neck muscles to maintain their postures for impact decelerations inattentively or attentively. Therefore, activation level of each neck muscle should be estimated to predict head-neck responses during rear impacts. In controlling activation level of each muscle to achieve an objective motion or posture, the calculation method such as optimization needs to repeat simulations with try and error. Therefore, computational cost for one cycle simulation should be reduced. We newly developed a musculo-skeletal FE model of elderly AF05 in a simple form that the skeletal parts were modeled by rigid bodies and the articulated joints were modeled with mechanical joints in addition to muscles modeled by only bar elements. The model was created by scaling down a musculo-skeletal FE model of AM50, which we developed previously (Iwamoto et al. 2012), to adjust the size of AF05. The model includes 8 cervical joints including C7-T1 joint and 23 neck muscles such as Longus Colli and Splenius Capitis. Each joint was modeled with a non-linear torque-angle property obtained from the literature (Panjabi et al. 1976). Since Kuhlman et al. (1993) reported that the cervical range of motion in elderly females with ages from 70 to 90 years old was 27 % smaller than that of young adult males with ages from 20 to 30 years old, we changed the non-linear torque angle property of the musculo-skeletal FE model of elderly AF05 to represent the difference. Each muscle was modeled using Hill type muscle material (LS-DYNA Material type 156, MAT_MUSCLE) with the maximum contraction force, passive and active force-elongation curves, and an active force-velocity curve obtained from Thelen et al. (2003). The PCSA of each muscle of the elderly female described in Table 1 was inputted to the corresponding muscle of the musculo-skeletal FE model of elderly AF05. Each muscle was connected with tendons at both sides of the muscle, which formulated muscle paths between the origin and the insertion points. The tendons were modeled with tension only non-linear stress-strain curves (LS-DYNA Material type B01, MAT_SEATBELT). The muscle included only one bar element (actually truss element) while the tendons included multiple seatbelt elements with a via-point on each side to represent muscular alignments and moment arm of the muscle based on anatomical references (Neumann, 2002). As a result, the 23 neck muscles included 90 muscular lines with bar elements and seatbelt elements on right side of head-neck region. For the simplicity of the musculo-skeletal FE model, no other tissues including skin and flesh, which might change the muscle paths and magnitudes of moment arms, were

directly represented in this study, because the musculo-skeletal FE model consisting of skeletal parts, joints, and muscles was supposed to be enough to represent gross motions of human body during impacts. In this study, the head rotational angle can be calculated as a rotational angle change around the head C.G.. The rotational angle corresponds to a rotational angle change of a line through the head C.G. that is parallel to the Frankfurt-plain line connecting infraorbitale to the external auditory meatus.

Authors previously proposed the reinforcement motion learning model with the synergy control policy between multiple muscles, which is modeled on the multiple muscle control function of Corticospinal motoneurons in cerebral cortex (Min et al., 2012). This model can robustly control the motion against external force. Based on this model, the system applied to the whole human body FE model was developed for estimating occupant motions and impact responses in crash situations (Iwamoto et al. 2012). The reinforcement learning (RL) is controlled in basal ganglia, which plays an important role for posture maintenance (Takakusaki et al., 2003). For accurate estimation of occupant postures in various occupant conditions including inattentive and attentive conditions under inertial environments with impact decelerations, the proposed learning model could be useful. Figure 16 shows a muscle control system for head-neck posture stabilization using this learning model. The system was developed using C++ program. The system produces control function of each muscle around a pre-determined articulated joint to hold the posture on a pre-determined target position. Three steps are necessary to perform the muscle control simulations under the inertial environments. Firstly, joint angle range and joint angular velocity range around a pre-determined target joint angle of 0 degree, should be determined, which were set to a range from -80 to 80 degrees and a range from -1600 to 1600 degrees/sec in this paper, respectively. The system provides the head C.G. with a boundary prescribed motion to rotate the head with the range around the head C.G.. Since each vertebra is connected by the associated articulated joints in the head-neck region, each vertebra in the head-neck region can rotate by the rotation around the head C.G.. Then the system creates a database including positions of the skeletal part, the joint, and muscle bar elements within the joint angle range. Secondly, after initial angle is randomly determined among the joint angle range, activation level of each muscle randomly generated by agent of RL is transferred to the muscle of a musculo-skeletal FE model via an interface, and then the musculo-skeletal FE model performs a motion around the joint using LS-DYNA. As a result, the information on the position, joint angle, and velocities of the joint and a target point is transferred to the agent via the interface. Then, the agent estimates the muscle control function as feedback controller, which outputs activation level of the muscle with the motion state consisting of joint angle and joint angular velocity (cf. Figure 16). This routine is repeated until stably controlling the motion for a goal with learning the optimal control policy. Thirdly, under an impact deceleration condition, activation level of each muscle obtained by inputting the current joint angle and joint angular velocity to the optimal control function of the muscle is given to the muscle model so that the human body motion is estimated. The detailed description of this learning model is found in the authors publications (Iwamoto et al.2012, Min et al. 2012).

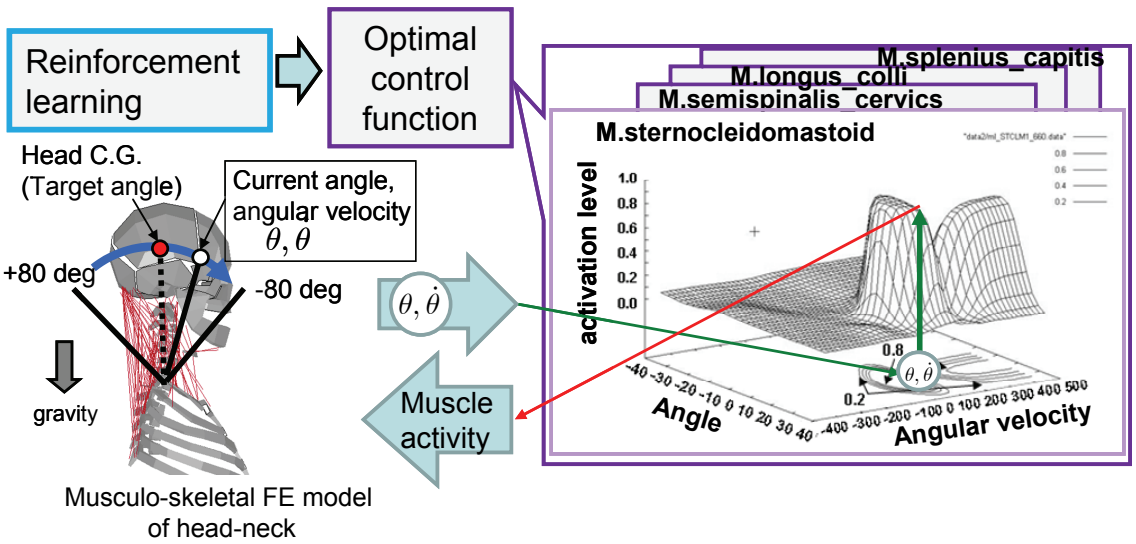

Figure 16. Muscle control system for head-neck posture stabilization using RL

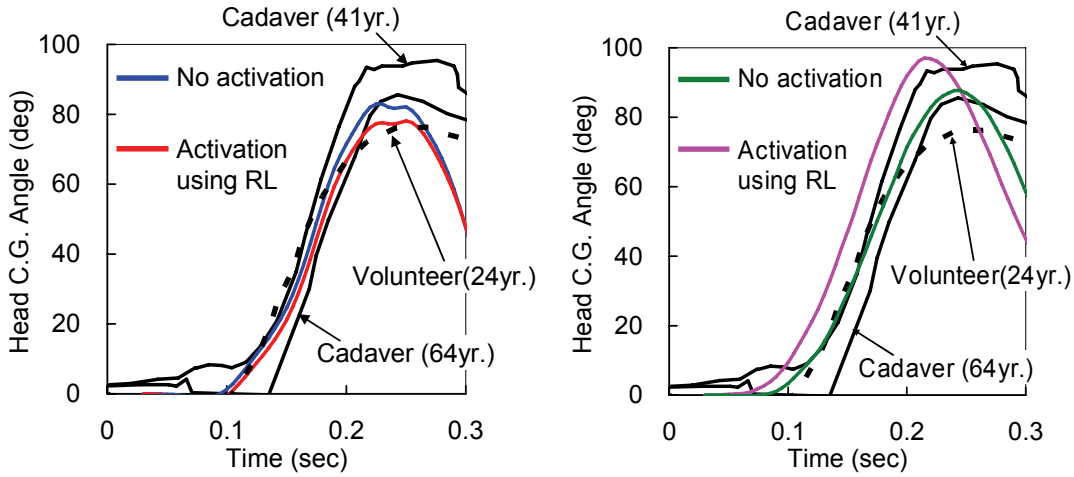

(a) Musculo-skeletal model (b) Muscular solid model

Figure 17. Head C.G. angle time histories in low-speed rear impact simulations using elderly AF05 model with and without muscle activation.

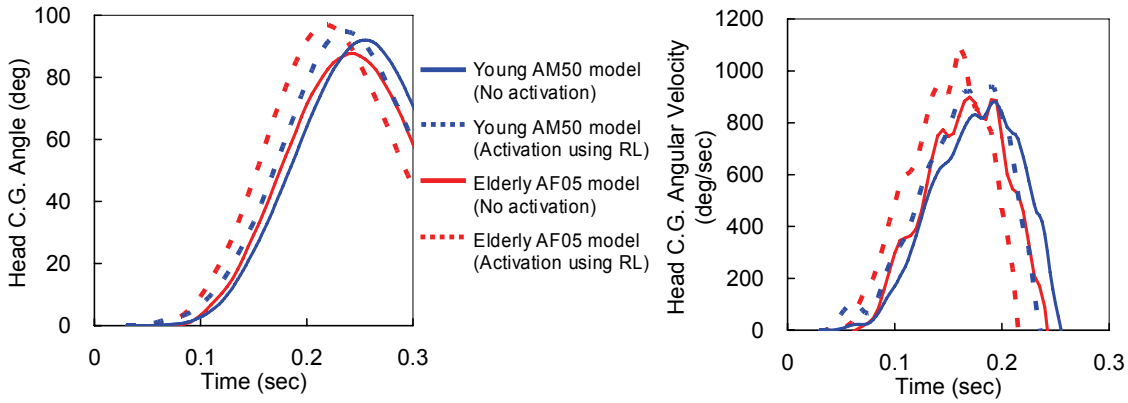

(a) Head C.G. angle (b) Head C.G. angular velocity

Figure 18. Comparison of time histories of head C.G. angle and angular velocity (Muscular solid model).

The musculo-skeletal FE model of elderly AF05 and the muscle controller with the proposed motion learning model were used for estimation of head-neck responses during a rear impact with a velocity of 8km/h as described previously. Figure 17(a) shows comparison of head C.G. rotational angle between simulation results and experimental test data. Figure 17(a) includes simulation results using the elderly AF05 model without activation and with activation levels obtained from the muscle controller.

Figure 17(a) also includes two cadaver test data obtained from White et al. (2009) and one volunteer test data obtained from Ono et al. (1997). The peak head C.G. angle of simulation result without muscle activation was close to that of elderly cadaver test data while the peak head C.G. angle of simulation result with RL was close to that of the volunteer test data. Muscle activation decreased the peak head C.G. angle by 5.0 degrees. The muscle activation level of each muscle obtained from the muscle controller was inputted to the corresponding muscle of the elderly AF05 model with the muscular solid elements shown in Figure 12(a), hereafter called muscular solid model, in the rear impact simulations. The activation level was also inputted to the muscular solid model of young adult AM50 to investigate aging effect of muscular forces for impact responses. Figure 17(b) shows comparison of head C.G. rotational angle between simulation results using the elderly AF05 model with and without activation. The peak head C.G. angle of simulation result of muscular solid model was close to that of musculo-skeletal model in the case without activation. On the other hand, the peak head C.G. angle of muscular solid model was different from that of musculo-skeletal model in the case with activation. This inconsistency is due to difference in modeling muscles and joints between two models of musculo-skeletal model and muscular

solid model. Figure 18 shows comparisons of time histories of head C.G. angle and angular velocity among four simulation results of the elderly AF05 model and the young adult AM50 model with and without activation. The head rotated earlier in the elderly AF05 model with activation than in the young adult AM50 model with activation by 22 msec. This is because the peak head C.G. angular velocity of the elderly AF05 model with activation were the largest among the four simulations, and was larger than the young adult AM50 model with activation by 158 degrees/sec as shown in Figure 18(b). The simulation results suggest that weak muscular forces of the elderly AF05 model with smaller PCSA could rotate the head rearward easily during rear impacts.

CONCLUSIONS

Elderly female occupants are most susceptible to injuries, especially on thorax and head-neck regions, based on previous studies using automotive accident data. This study developed a finite element (FE) model of 5th percentile female (AF05) with multiple muscles, and inputted material properties of elderly people to bones in ribcage and lower extremities, cervical spine discs, muscles of whole body to elucidate injury mechanism of elderly female occupants.

The developed elderly AF05 model was firstly validated against some cadaver test data on thoracic deformation in frontal impacts and head-neck responses in a low-speed rear impact. The model was secondly used for investigation on effect of muscle activation for the impact responses. Several comparisons between the elderly AF05 model and the young adult AM50 model showed that lower strength of bones and smaller PSCA of each muscle in the elderly AF05 could increase thoracic deflection. Those comparisons also suggest that the elderly AF05 could not prevent the head from rotating rearward due to the weak muscular forces compared with the young adult AM50.

Although the elderly AF05 model has some limitation on lack of experimental data for validations and the inconsistency in human body kinematics between the musulo-skeletal FE model and the muscular solid model, it has a promising tool for better understanding of injury mechanisms of elderly female occupants.

REFERENCES

[1] Agur, A.M.R., Dalley II, A.F. 2005. Grant's Atlas of Anatomy; 11th Edition, Lippincott Williams & Wilkins, Baltimore, Maryland.

[2] Begeman, P., King, A.I., Levine, R., Viano, D.C. 1980. "Biodynamic Response of the Musculoskeletal System to Impact Acceleration" Stapp Car Crash Conference, No.801312, 479-509.

[3] Behr, M., Arnoux, P-J., Serre, T., Thollon, L., Brunet, C. 2006. "Tonic Finite Element Model of the Lower Limb" Journal of Biomechanical Engineering, Vol. 128, 223-228.

[4] Bougie, J.D., Morgenthal, A.P. 2001, The Aging Body: conservative care for common neuromusculoskeletal conditions, McGraw-Hill Companies, Inc.

[5] Brolin K. 2003, "Neck injuries among the elderly in Sweden", Injury Control and Safety Promotion, Vol.10, No.3, 155-164.

[6] Brumbelow, M. L., Zuby, D.S. 2009. "Impact and Injury Patterns in Frontal Crashes of Vehicles with Good Ratings for Frontal Crash Protection", 21st ESV Conference, No.09-0257.

[7] Carlson, G.D., Botte, K.J., Josephs, M.S., Newton, P.O., Davis, J.L.W., Woo, S.L-Y. 1993. "Morphologic and biomechanical comparison of tendons used as free grafts", Journal of hand surgery, Vol.18A, No.1, 76-82.

[8] Ejima, S., Zama, Y., Ono, K., Kaneoka, K., Shiina, I., Asada, H. 2009. "Prediction of Pre-Impact Occupant Kinematic Behavior Based on the Muscle Activity during Frontal Collision" 21st ESV Conference, No.09-0913.

[9] El-Jawahri, R.E., Laituri, T.R., Ruan, J.S., Rouhana, S.W., Barbat, S.D. 2010, "Development and Validation of Age-Dependent FE Human Models of a Mid-Sized Male Thorax, Stapp Car Crash Journal, Vol.54, 407-430.

[10] Gans, C. 1982. "Fiber architecture and muscle function" Exercise and Sports Sciences Reviws, 10, 106-107.

[11] Institute for Traffic Accident Research and Data Analysis, 2007, "Accident injury of elderly drivers of four wheel vehicles", ITARDA Information, No.71, (in Japanese)

[12] Ito, O., Dokko, Y., Ohashi, K. 2009, "Development of Adult and Elderly FE Thorax Skeletal Models", SAE Paper, No.2009-01-0381.

[13] Iwamoto, M., Kisanuki, Y., Watanabe, I., Furusu, K., Miki, K., Hasegawa, J. 2002. "Development of a Finite Element Model of the Total Human Model for Safety (THUMS) and Application to Injury Reconstruction" IRCOBI Conference, 31-42.

[14] Iwamoto, M., Nakahira, Y., Tamura, A., Kimpara, H., Watanabe, I., Miki, K. 2007, "Development of Advance Human Models in THUMS", Proc.6th European LS-DYNA Users' Conference. 47-56.

[15] Iwamoto, M., Nakahira, Y., Sugiyama, T. 2011, "Investigation of pre-impact bracing effects for injury outcome using an active human FE model with 3D geometry of muscles, 22nd ESV Conference, No.11-0150.

[16] Iwamoto, M., Nakahira, Y., Kimpara, H., Sugiyama, T., Min, K. 2012, "Development of a

Human Body Finite Element Model with Multiple Muscles and their Controller for Estimating Occupant Motions and Impact Responses in Frontal Crash Situations", Stapp Car Crash Journal, Vol.56, 231-268.
[17] Kemper, A. R., McNally, C., Kennedy, E. A., Manoogian, S. J., Rath, A. L., Ng, T. P., Stitzel, J. D., Smith, E. P., Duma, S. M. 2005, "Material properties of human rib cortical bone from dynamic tension coupon tenting". Stapp Car Crash Journal, vol.49, 199-230.
[18] Kent, R., Lessley, D., Sherwood, C. 2004. "Thoracic Response to Dynamic, Non-Impact Loading from a Hub, Distributed Belt, Diagonal Belt, Double Diagonal Belts" Stapp Car Crash Journal, Vol.48, 495-519.
[19] Kimpara, H., Lee, J.B. Yang, K.H., King, A.I. Iwamoto, M., Watanabe, I., Miki, K. 2005, "Development of a Three-Dimensional Finite Element Chest Model for the 5th Percentile Female", Stapp Car Crash Journal, Vol.49, 251-269.
[20] Krafft, M., Kullgren, A., Lie, A., Tingvall C. 2003, "The risk of whiplash injury in the rear seat compared to the front seat in rear impacts", Traffic Inj. Prev., Vol.4, No.2, 136-140.
[21] Kroell, C. K., Schneider, D. C., and Nahum, M.1971, "Impact Tolerance and Response of the Human Thorax", SAE Paper No. 710851.
[22] Kuhlman, K.A.1993, "Cervical range of motion in the elderly", Arch. Phys. Med. Rehabil. Vol.74, 1071-1079.
[23] Liu,C., Utter, D., Chen. C.-L. 2007, "Characteristics of Crash Injuries Among Young, Middle-Aged, and Older Drivers", NHTSA Technical Report, No. DOT HS 810 857.
[24] Malik, S.A., Murphy, M., Connolly, P., O'Byrne, J. 2008, "Evaluation of morbidity, mortality and outcome following cervical spine injuries in elderly patients", Eur. Spine. J., 17, 585-591.
[25] Min, K., Kimpara, H., Iwamoto, M. 2012, "Load Response Simulation of Human Arm Musculo-Skeletal FE Model with the Learning of Muscle Synergy Control Policy", Neural Networks, submitted, 2012.
[26] National Institute of Population and Social Security Research, 2012, "Population projection for Japan in 2011-2060" (in Japanese)
[27] Neumann, D.A. 2002, Kinesiology of the Musculoskeletal System: Fundations for Physical Rehabilitation, Mosby Inc.
[28] Nusholtz, G., and Kaiker, P. 1994, "Abdominal Response to Steering Wheel Loading", Proc. the 14th ESV Conference, 118-127.
[29] Ono, K., Kaneoka, K., Wittek, A., Kajzer, J. 1997, "Cervical Injury Mechanism Based on the Analysis of Human Cervical Vertebral Motion and Head-Neck-Torso Kinematics during Low Speed Rear Impacts", Proc. of the 41st Stapp Car Crash Conference, 973340, 339-356.
[30] Panjabi, M.M., Brand, R.A., White, A.A.1976, "Mechanical Properties of the Human Thoracic Spine", The Journal of Bone and Joint Surgery, 642-652.
[31] Rosen, C.J., Glowacki, J., Bilezikian, J.P. (eds.) 1999, The Aging Skeleton, Academic Press
[32] Simamura, M., Ohhashi, H., Yamazaki, M. 2003. "The Effects of Occupant Age on Patterns of Rib Fractures to Belt-Restrained Drivers and Front Passengers in Frontal Crashes in Japan" Stapp Car Crash Journal, Vol.47, 349-365.
[33] Snyder, R.G., Chaffin, D.B., Foust, D.R. 1975. "Bioengineering Study of Basic Physical Measurements Related to Susceptibility to Cervical Hyperextension-Hyperflexion Injury, UM-HSRI-BI-75-6.
[34] Stalnaker, R.L., McElhaney, J.H., Roberts, V.L., Trollope, M.L.1973, "Human Torso Response to Blunt Trauma, Human Impact Response, Measurement and Simulation", 181-199, PLENUM PRESS, New York-London.
[35] Takakusaki, K., Habaguchi, T., Ohtinata-Sugimoto, J., Saitoh, K., Sakamoto, T. 2003, "Basal Ganglia Efferents to the Brainstem Centers Controlling Postural Muscle Tone and Locomotion: A New Concept for Understanding Motor Disorders in Basal Ganglia Dysfunction", Neuroscience, 119, 293-308.
[36] The General Insurance Association of Japan, 2004, "Current and future state of automotive accidents involving senior drivers" (in Japanese)
[37] Thelen, D. G. 2003. "Adjustment of Muscle Mechanics Model Parameters to Simulate Dynamic Contractions in Older Adults" Transaction of the ASME, Vol.125.
[38] White, N.A. Begeman, P.C., , Hardy, W.N., Yang, K.H., Ono, K., Sato, F., Kamiji, K., Yasuki, T., Bey, M.J. 2009, "Investigation of Upper Body and Cervical Spine Kinematics of Post Mortem Human Subjects (PMHS) during Low-Speed, Rear-End Impacts", SAE 2009-01-0387.
[39] Winters, J.M. 1990. "Hill-Based Muscle Models" A System Engineering Perspective; Multiple Muscle Systems: Biomechanics and Movement Organization, Winters, J.M. and Woo. S. (eds.), New York, Springer, 69-93 and 726-749.
[40] Yaguchi, M., Omoda, Y., Ono, K., Masuda, M., Onda, K. 2011, "Traffic accident analysis towards the development of an advanced frontal crash test dummy indispensable for further improving vehicle occupant protection performance", 22nd ESV Conference, No. 11-0221.
[41] Yamada, H. 1970. Strength of Biological Materials; Williams & Wilkins Company.
[42] Yee, W.Y., Cameron, P.A., Bailey, M.J. 2006, "Road traffic injuries in the elderly", Emerg. Med., J. 23, 42-46.